Hindawi
Mathematical Problems in Engineering
Volume 2018, Article ID 9208568, 7 pages
https://doi.org/10.1155/2018/9208568

Research Article

Wideband Sparse Signal Acquisition Based on Serial Multi-Coset Sampling

Changjian Liu and Houjun Wang

School of Automation Engineering, University of Electronic Science and Technology of China, Chengdu 611731, China

Correspondence should be addressed to Changjian Liu; changjian.liu@outlook.com

Received 9 February 2018; Accepted 20 May 2018; Published 3 July 2018

Academic Editor: Dragan Poljak

Traditional parallel multi-coset sampling (MCS), which has several sub-Analog-to-Digital-Converters (sub-ADCs) working parallelly, is an attractive sub-Nyquist sampling technique for wideband sparse signals. However, the mismatch among sub-ADCs in traditional parallel MCS, such as bias, gain, and timing skew mismatch, degrades the signal acquisition performance greatly. In this paper, a serial MCS scheme based on clocking single ADC with nonuniform clock is proposed. The nonuniform sampling clock is generated by a pseudo-random binary sequence generator. An additional Sample/Hold (S/H) is used to improve the analog bandwidth of the serial MCS. Moreover, universal sampling pattern is designed for the proposed serial MCS. The sampling pattern design should not only maximize the Kruskal rank of compressed sensing matrix but also take the ADC's sub-Nyquist sampling rate into consideration. Numeral experiments are presented demonstrating that the mismatch among sub-ADCs in traditional parallel MCS degrades the reconstruction performance greatly, and the proposed serial MCS can avoid the mismatch tactfully.

1. Introduction

Wideband sparse signal is also called a multiband signal. Its frequency support concentrates on several continuous intervals and is distributed over a wide spectrum [1]. The multiband signal can be found in many applications such as communication and radar. For example, communication signal is the summation of several modulated signal with different baseband signal and carrier frequency. According to the Nyquist sampling theorem, the sampling rate required for multiband signal may exceed several times of the state-of-the-art Analog to Digital Converter's (ADC) sampling rate.

The joint sparsity of multiband signal can be utilized to reduce the sampling rate requirement. Several sub-Nyquist sampling techniques have been proposed to acquire multiband signal at a sub-Nyquist rate [1–9]. Compared with the Modulated Wideband Converter (MWC) [2], multi-coset sampling (MCS) is more attractive because using pseudo-random binary sequence as the local oscillator signal of a mixer will generate a lot of unwanted harmonics in MWC. Multi-coset sampling can be implemented on time-interleaved ADC (TIADC) platform to further enhance its time resolution. Compared with the traditional uniform sampling, MCS is an undersampling technique. Its overall sampling rate can be less than the Nyquist rate, so it can reduce the cost of sampling circuit in terms of price and power consumption. However, the mismatch among sub-ADCs in TIADC, such as bias, gain, and timing skew mismatch, is still a problem for multi-coset sampling [10, 11]. Moreover, temperature variation and aging may aggravate the mismatch continuously.

In this paper, a serial multi-coset sampling scheme based on clocking single ADC with nonuniform clock is proposed. The nonuniform clock is generated by the pseudo-random binary sequence generator. An additional Sample/Hold (S/H) is used to improve the analog bandwidth of the proposed serial MCS. Moreover, universal sampling pattern is designed for the proposed serial MCS. The sampling pattern design should not only maximize the Kruskal rank of compressed sensing matrix but also take the ADC's sub-Nyquist sampling rate into consideration. Although the sampling rate requirement of the ADC based on the proposed serial MCS is higher than that of the traditional parallel MCS, the proposed MCS does not exist channel mismatch problem and its size is

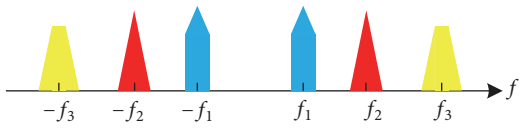

Figure 1: Typical wideband sparse signal.

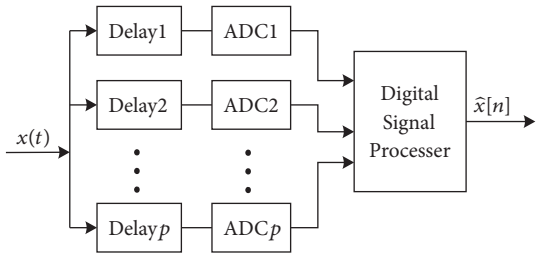

Figure 2: Block diagram of the traditional parallel MCS.

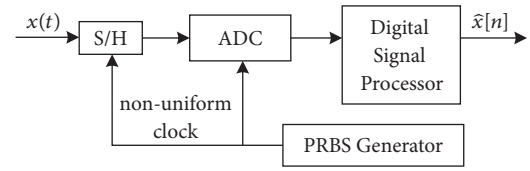

Figure 3: Block diagram of the proposed serial MCS.

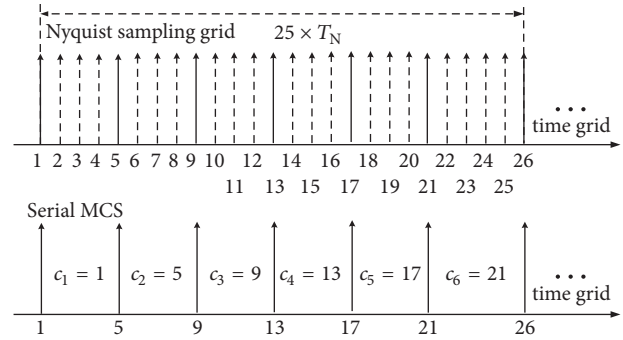

Figure 4: Sampling process of the proposed serial MCS.

smaller. Numeral experiments are presented demonstrating the proposed serial MCS has a better reconstruction performance than the traditional parallel MCS.

1.1. Signal Model and Problem Statement. Let $x(t)$ denote the real-valued and squared integrable multiband signal. It is assumed to bandlimited to $\mathscr{R} = [-f_N/2, +f_N/2]$, where f_N is the Nyquist sampling rate of the input signal. Let T_N denote the Nyquist sampling interval. The Fourier transform of $x(t)$ can be written as

$$X(f) = \int_{-\infty}^{\infty} x(t) \exp(-j2\pi ft)\, dt. \quad (1)$$

The frequency support of $X(f)$ concentrates on several subbands whose maximal bandwidth is B. Let M denote the number of subbands within $X(f)$ and it is even because of the conjugate symmetry property of a real signal's Fourier transform. These subbands are randomly distributed over $\mathscr{R}$ and their position is unknown beforehand. Figure 1 shows a typical wideband sparse signal with $M = 6$ subbands.

We wish to design a sampling system and it should have the following properties: first, sampling rate requirement should be as low as possible; second, the position of active subbands is not available beforehand for both the sampling and reconstruction stage; third, the proposed sampling system is supposed to only use currently available integrated circuits.

1.2. Traditional Parallel Multi-Coset Sampling. Let $x(nT_N)$, $1 \le n \le \infty$ be the sequence of samples obtained at the Nyquist sampling rate. In MCS, $x(nT_N)$ is divided into blocks of length L and only $p < L$ samples are acquired. The selection of p samples from L samples is determined by the sampling pattern $C = \{c_1, c_2, \ldots, c_p\}$, where $1 \le c_1 \le \cdots \le c_p \le L$.

Figure 2 shows the traditional method to implement multi-coset sampling. It can be implemented on a time-interleaved ADC platform by only implementing p out of L sub-ADCs. So the overall system sampling rate is $(p/L) \times f_N$ which is lower than the Nyquist rate f_N since (p/L) is smaller than 1. The input signal is first delayed by different time $c_i T_N$ and then sampled by the following ADC with sampling rate f_N/L. The effect of delay can be realized via delaying the sampling clock. The mismatch among sub-ADCs, such as bias, gain, and timing skew mismatch, will deteriorate the signal reconstruction performance of TIADC, so does the multi-coset sampling system. Although many methods have been proposed to compensate the mismatch [10, 11], this will bring about a large amount of work on calibration.

2. Serial Multi-Coset Sampling

2.1. Description of the Proposed Serial Multi-Coset Sampling. An overview of the proposed serial MCS is shown in Figure 3. The S/H is used to enhance analog bandwidth of serial MCS since analog bandwidth of an ADC is usually not enough. The input signal is first sampled by S/H, and then the following ADC quantizes the output of S/H. Pseudo-random binary sequence (PRBS) generator can be used to generate the nonuniform sampling clock. The sampling pattern C determines the generation of nonuniform clock. Several sequences of uniform samples can be obtained after classifying and dividing the single sequence of nonuniform samples. An example of the sampling process is shown in Figure 4 in which $p = 6$, $L = 25$ and $C = \{1, 5, 9, 13, 17, 21\}$.

Let N_0 denote the number of samples per coset and the total number of nonuniform samples is $N = p \times N_0$. Let $\boldsymbol{y}[n]$, $1 \le n \le N$ be the nonuniform samples and it can be written as

$$\boldsymbol{y}[n] = \left[y_{c1}[1], y_{c2}[2], \ldots, y_{cp}[p], y_{c1}[1+p], \ldots\right]. \quad (2)$$

Then the sequence of nonuniform samples $\boldsymbol{y}[n]$, $1 \le n \le N$ can be classified and divided into p sequences of uniform samples:

$$\boldsymbol{y}_{ci}[k] = \boldsymbol{y}[k \times L + c_i], \tag{3}$$

where $1 \le i \le p$ and $0 \le k \le N_0 - 1$. Let $\boldsymbol{y_{ci}} = [y_{ci}[0], y_{ci}[1], \ldots, y_{ci}[N_0 - 1]]^T$ represent the i-th sequence of uniform samples. The sampling rate of $\boldsymbol{y_{ci}}$ is f_N/L and the time offset of $\boldsymbol{y_{ci}}$ is $ci \times T_N$. p sequences of uniform samples can be written in matrix form concisely:

$$\boldsymbol{y} = \left[\boldsymbol{y_{c1}}, \boldsymbol{y_{c2}}, \ldots, \boldsymbol{y_{cp}}\right]^T. \tag{4}$$

For practical application consideration, the nonuniform sampling clock is provided by a pseudo-random binary sequence generator. The current state-of-the-art PRBS generator can reach alteration rate of 80GHz [1]. The requirement for S/H's analog bandwidth is high but the requirement for the following ADC's analog bandwidth is low. The analog bandwidth and sampling rate of the current state-of-the-art S/H product are 18GHz and 4GSPS (Giga Sample Per Second), respectively (HMC760LC4B, Analog Devices, Inc.). When the sampling setting in Figure 4 is adopted, the proposed scheme can acquire wideband sparse signal in the frequency range [DC-1GHz] using a S/H with 1GHz analog bandwidth and 480MSPS sampling rate and an ADC with sampling rate 480MSPS.

The output voltage of S/H drifts slowly when it is in the hold mode. The drift is caused by the current leakage of the hold capacitor of the S/H, and the output voltage of S/H decays as the hold time increases. According to the datasheet of S/H (HMC760LC4B), the drift consists of two parts. One part is fixed, and the other part has a linear relationship with the hold voltage. The total drift can be approximated by $D = D_0 + D_{\text{lin}}V_{\text{in}}$, where D_0 is the fixed part, D_{lin} is the linear drift factor, and V_{in} is the hold voltage. Since the nonuniform sampling clock provided to ADC is a delayed version of the nonuniform sampling clock provided to S/H, the hold time for each sample is the same. So the linear drift factor D_{lin} is the same for each sample. On the other hand, the fixed part of the drift D_0 is small compared with the linear distortion part $D_{\text{lin}}V_{\text{in}}$ according to the datasheet of HMC760LC4B. Therefore, the drift will result in little nonlinear distortion.

The proposed serial MCS has a higher sampling rate requirement for the ADC than the traditional parallel MCS. The sampling rate requirement for ADC is $f_{\text{ADC}} \ge p \times f_N/L$ in serial MCS. Although the requirement for sampling rate is higher, there is no bias, gain, and timing skew mismatch in serial MCS.

2.2. Reconstruction from p Sequences of Uniform Samples. The connection between the continuous time Fourier transform of input signal $X(f)$ and the discrete time Fourier transform of the i-th sequence of uniform samples $\boldsymbol{y}_{ci}(e^{j2\pi f T_N})$ can be written as follows [1]:

$$\boldsymbol{y}_{ci}\left(e^{j2\pi f T_N}\right) = \frac{f_N}{L}\sum_{r=0}^{L-1} e^{j(2\pi/L)ir} X\left(f + \frac{f_N r}{L}\right), \quad f \in \mathscr{F}_0, \tag{5}$$

where $1 \le i \le p$ and $\mathscr{F}_0 = [0, 1/(LT_N))$. p linear equations can be written in matrix form conveniently:

$$\boldsymbol{y}(f) = \mathbf{A}\boldsymbol{x}(f) \quad \forall f \in \mathscr{F}_0, \tag{6}$$

where $\boldsymbol{y}(f)$ is a $p \times 1$ vector whose i-th element is $\boldsymbol{y}_{ci}(e^{j2\pi f T_N})$, $\mathbf{A}$ is a $p \times L$ matrix whose ir-th element is given by $\mathbf{A}_{ir} = \exp(j2\pi ir/L)/(L \times T_N)$, $L \times 1$ vector $\boldsymbol{x}(f)$ contains L unknowns for each f and $\boldsymbol{x}_i(f) = X(f + i/(LT_N))$, $0 \le i \le L - 1$, $f \in \mathscr{F}_0$. The frequency support S of $X(f)$ can be estimated by continuous-to-finite (CTF) algorithm [1], then the previous under-determined problem (6) can be transformed into an overdetermined problem:

$$\boldsymbol{y}(f) = \mathbf{A}_S \boldsymbol{x}^S(f) \quad \forall f \in \mathscr{F}_0. \tag{7}$$

Eventually, least square estimator can be utilized to solve the overdetermined problem (7). The time-domain data of input signal can be obtained through inverse Fourier transform after the spectrum has been recovered.

3. Universal Sampling Pattern Design

The frequency support of $x(t)$ is unknown for both the sampling stage and reconstruction stage. Continuous-to-finite algorithm can be used to find the frequency support and it requires that $x(f)$ is $\text{K}(\mathbf{A})/2$ sparse for $f \in \mathscr{F}_0$. $\text{K}(\mathbf{A})$ is the Kruskal rank of a matrix $\mathbf{A}$ and it is defined as the maximal number q such that every q columns are linearly independent [1].

A sampling pattern C is called a universal sampling pattern if the Kruskal rank $\text{K}(\mathbf{A})$ of the compressed sensing matrix $\mathbf{A}$ in (6) is equal to the cardinality of the sampling pattern $|C|_0$. The design of sampling pattern is very important because we want to maximize the set of signal that the serial MCS can acquire.

From the above description, the selection of C from $\{1, 2, \ldots, L\}$ should be paid special attention to. The following theorem provides a method to design a universal sampling pattern for serial MCS.

Theorem 1. *Let the sampling pattern $C = \{c_1, c_2, \ldots, c_p\}$ be chosen from $\{1, 2, \ldots, L\}$ and $c_i = c_1 + (i-1)d$, which is an arithmetic progression with difference d. The $p \times L$ matrix $\mathbf{A}$ is defined in (6). Then*

$$\text{K}(\mathbf{A}) = p \Longleftrightarrow \begin{cases} d \text{ and } L \text{ are coprime} \\ d \ge \left\lceil \dfrac{f_N}{f_{ADC}} \right\rceil. \end{cases} \tag{8}$$

Proof. Matrix $\mathbf{A}$ is a Vandermonde matrix and it can be written as

$$\mathbf{A} = \begin{pmatrix} 1 & \alpha_1 & \alpha_1^2 & \cdots & \alpha_1^{L-1} \\ 1 & \alpha_2 & \alpha_2^2 & \cdots & \alpha_2^{L-1} \\ \vdots & \vdots & \vdots & \ddots & \vdots \\ 1 & \alpha_p & \alpha_p^2 & \cdots & \alpha_p^{L-1} \end{pmatrix}, \tag{9}$$

where $\alpha_i = e^{j2\pi c_i/L} = e^{j2\pi(c_1+(i-1)d)/L} = \alpha_1\alpha^{(i-1)d}$, $\alpha_1 = e^{j2\pi c_1/L}$ and $\alpha = e^{j2\pi/L}$. $\mathbf{A}$ can be further written as

$$\mathbf{A} = \begin{pmatrix} 1 & \alpha_1^1 & \cdots & \alpha_1^{L-1} \\ 1 & \alpha_1^1\alpha^{1d} & \cdots & \alpha_1^{L-1}\alpha^{(L-1)d} \\ \vdots & \vdots & \ddots & \vdots \\ 1 & \alpha_1^1\alpha^{1(p-1)d} & \cdots & \alpha_1^{L-1}\alpha^{(L-1)(p-1)d} \end{pmatrix}. \quad (10)$$

Since the independence of column vectors is investigated, the constant factor α_1^{i-1} in each column can be removed and then $\mathbf{A}$ can be written as

$$\mathbf{A} = \begin{pmatrix} 1 & 1 & \cdots & 1 \\ 1 & \alpha^{1d} & \cdots & \alpha^{(L-1)d} \\ \vdots & \vdots & \ddots & \vdots \\ 1 & \alpha^{1(p-1)d} & \cdots & \alpha^{(L-1)(p-1)d} \end{pmatrix}. \quad (11)$$

Matrix $\mathbf{A}$ can be viewed as a $p \times L$ row-wise Vandermonde matrix whose rows are the powers of $[1, \alpha^{1d}, \alpha^{2d}, \ldots, \alpha^{(L-1)d}]$. If elements in $[1, \alpha^{1d}, \alpha^{2d}, \ldots, \alpha^{(L-1)d}]$ are different from each other, then all columns are linearly independent, and the Kruskal rank of matrix $\mathbf{A}$ is p. So the situation when two elements are equal in $[1, \alpha^{1d}, \alpha^{2d}, \ldots, \alpha^{(L-1)d}]$ should be avoided and let i and j denote the index of elements which are equal. $\alpha^{id} = \alpha^{jd}$ can be further written as $\alpha^{(i-j)d} = 1 = \alpha^{cL}$. $(i-j)d = cL$, where $(i-j)$ and c are integers, denoting that d and L are not coprime. Therefore, d and L must be coprime. On the other hand, the sampling time interval between two sampling cosets should be greater than $1/f_{\mathrm{ADC}}$. So the minimum gap between two cosets or d should satisfy the following condition:

$$d \geq \left\lceil \frac{1/f_{\mathrm{ADC}}}{1/f_N} \right\rceil = \left\lceil \frac{f_N}{f_{\mathrm{ADC}}} \right\rceil. \quad (12)$$

□

4. Results and Discussion

The performance of the proposed serial MCS is evaluated with the following signal:

$$x(t) = \sum_{i=1}^{M/2} A_i \,\mathrm{sinc}\left(B\left(t - t_i\right)\right) \cos\left(j2\pi f_i t\right), \quad (13)$$

where $M/2$ denotes the number of subbands in $(0, f_N/2)$, A_i is the i-th band's energy coefficient and $A_i \sim \mathrm{U}(10, 50)$, B is the width of subband and it is set as $B = 40\mathrm{MHz}$, t_i is the i-th band's time offset and $t_i \sim \mathrm{U}(0, 2\mathrm{uS})$, and f_i is the i-th band's carrier frequency and $f_i \sim \mathrm{U}(0, 2\mathrm{GHz})$. In the following experiments, $f_N = 2\mathrm{GHz}$, $f_{\mathrm{ADC}} = 480\mathrm{MHz}$, $M = 6$ $L = 25$ and additive Gaussian noise is added to the original signal $x(t)$. Output Signal-to-Noise Ratio (SNR) is used as a metric to evaluate the proposed sampling scheme and it is defined as $\mathrm{SNR(dB)} = 20 \cdot \log_{10}(\|X(f)\|/\|X(f) - \widehat{X}(f)\|)$ where $X(f)$ and $\widehat{X}(f)$ denote the original spectrum without noise and reconstructed spectrum, respectively.

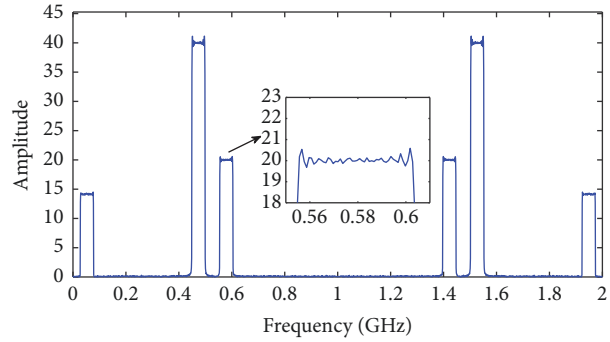

Figure 5: Original spectrum.

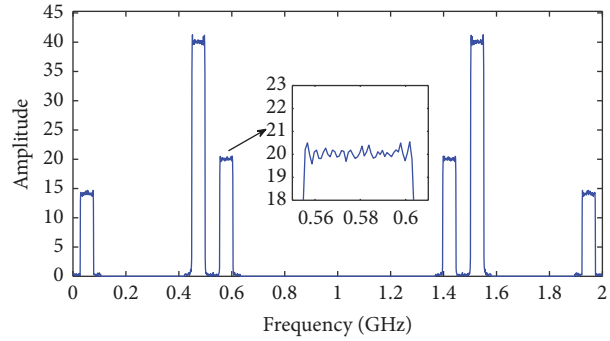

Figure 6: Reconstructed spectrum by proposed serial MCS.

In the first experiment, we test the feasibility of the proposed serial MCS. Reconstruction result is compared with the traditional parallel MCS. The mismatch parameters are set as follows: the timing skew mismatch is 2% of the Nyquist sampling interval; the bias and gain mismatch are both 2% of the maximal signal amplitude. Original signal spectrum is shown in Figure 5. The reconstruction results of the proposed serial MCS and traditional parallel MCS are shown in Figures 6 and 7, respectively. The spikes in Figure 7 are due to bias and gain mismatch while the large error in zoom window in Figure 7 is as a result of the timing skew. Although the sampling rate requirement for the ADC in serial MCS is higher, the mismatch among sub-ADCs in traditional parallel MCS can be avoided. The proposed serial MCS has a better reconstruction performance than the traditional parallel MCS.

In the second experiment, we investigate the reconstruction performance with respect to each kind of mismatch separately. 200 trials are performed for each experiment. Figures 8 and 9 show the influence of bias and gain mismatch, respectively, and they both vary from 0 to 10% of the maximal input signal's amplitude. Figure 10 shows the influence of timing skew mismatch and it varies from 0 to 10% of the Nyquist sampling interval. The reconstruction performance is tested in three SNR setting: 5dB, 10dB, and 15dB. It is shown in Figures 8–10 that the averaged output SNR decreases as the mismatch error increases. The reason is that the spikes'

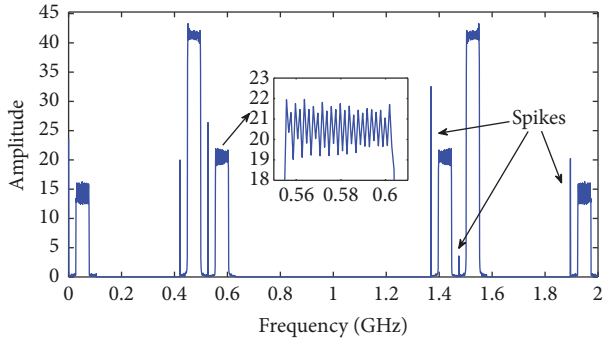

Figure 7: Reconstructed spectrum by traditional parallel MCS.

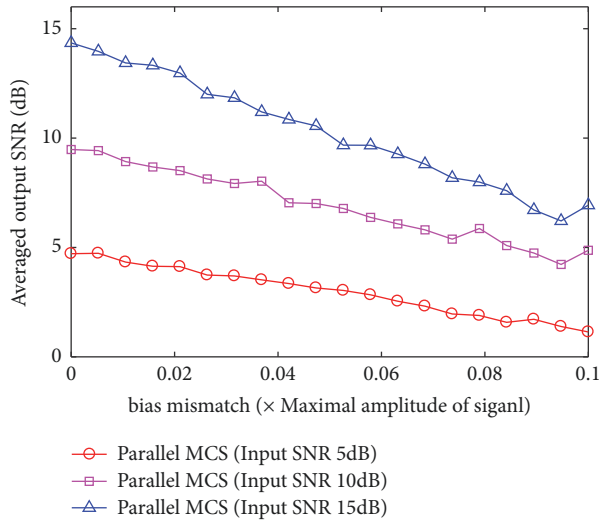

Figure 8: Reconstruction performance (only bias mismatch).

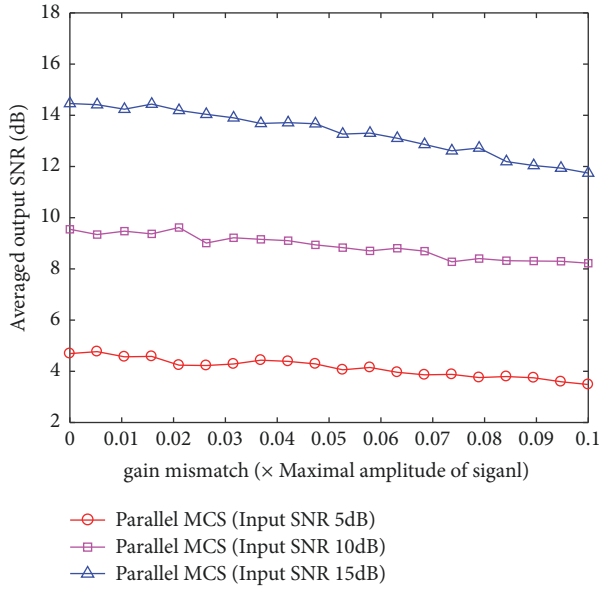

Figure 9: Reconstruction performance (only gain mismatch).

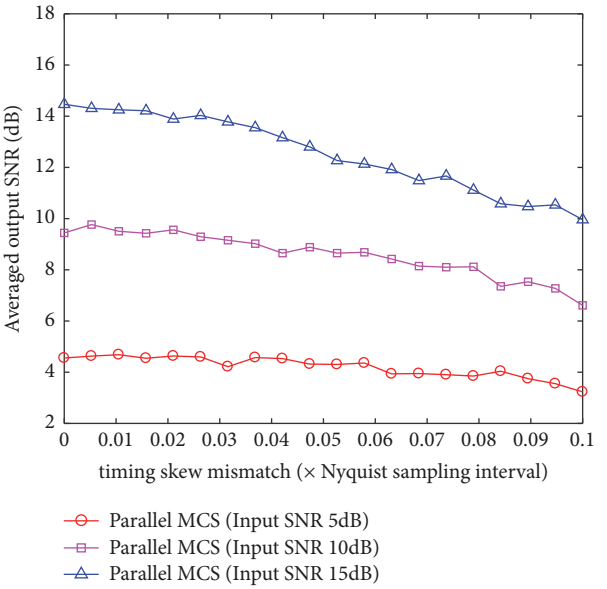

Figure 10: Reconstruction performance (only timing skew mismatch).

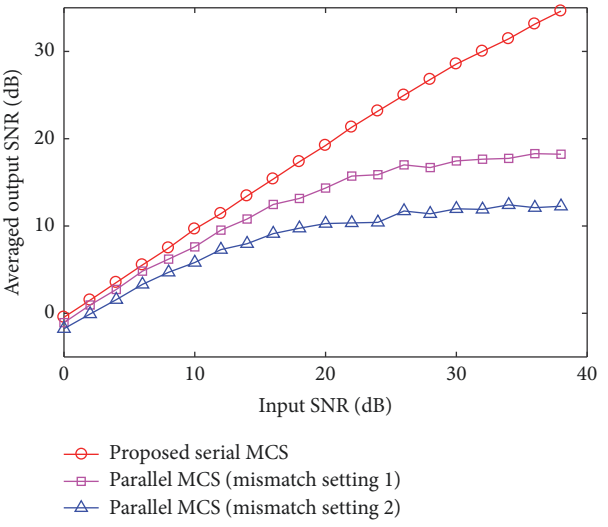

Figure 11: Reconstruction performance with respect to input SNR.

amplitude and the estimation error in the zoom window in Figure 7 increase with the increase of mismatch error.

In the third experiment, we investigate the reconstruction performance with respect to different input SNR over the range $[0, 38]$dB. In mismatch setting 1, the bias and gain mismatch are both set as 2% of the input signal's maximal amplitude, and the timing skew mismatch is set as 2% of the Nyquist sampling interval. In mismatch setting 2, the bias and gain mismatch are both set as 5% of the input signal's maximal amplitude, and the timing skew mismatch is set as 5% of the Nyquist sampling interval. It is shown in Figure 11 that the averaged output SNR linearly increases as the input SNR linearly increases for the proposed serial MCS. However, the averaged output SNR of the traditional

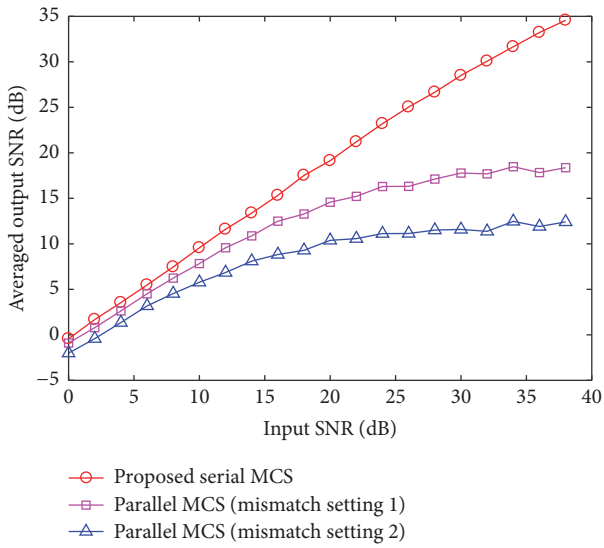

Figure 12: Reconstruction performance with respect to input SNR.

parallel MCS does not increase linearly as the input SNR linearly increases due to the mismatch among sub-ADCs in traditional parallel MCS. It is also shown in Figure 11 that, for input signal with low SNR, the mismatch has a little influence on the averaged output SNR. The reason is that the mismatch error is comparable to the noise amplitude in the low SNR setting. The proposed serial MCS has a better performance compared with the traditional parallel MCS when the input signal's SNR is greater than 10dB.

In the fourth experiment, in order to demonstrate the validity of the proposed MCS for other signal, Quadrature Phase-Shift Keying (QPSK) signal is used as the test signal. It is generated by the following model:

$$x(t) = E\sum_{k=1}^{M/2}\left\{\sum_{i=1}^{N_b} I_k[i]\, g_k(t - iT_k)\times\cos(2\pi f_k t) + \sum_{j=1}^{N_b} Q_k[j]\, g_k(t - jT_k)\times\sin(2\pi f_k t)\right\} + n(t), \tag{14}$$

where $M/2$ is the number of subbands in $(0, f_N/2)$, N_b is the number of random bits, $I_k[i]$ and $Q_k[j]$ are random bit streams, $g_k(t)$ is the pulse-shaping function, T_k is the symbol duration, f_k is the k-th band's carrier frequency and $f_k \sim U(0, 2\text{GHz})$, and $n(t)$ is the additive white Gaussian noise. The width of subband is set as 40MHz. The pulse-shaping function is the root-raised cosine with roll-over factor 0.1. $f_N = 2\text{GHz}$, $f_{ADC} = 480\text{MHz}$, $M = 6$, $L = 25$ and additive Gaussian noise $n(t) \sim \mathcal{N}(0, \sigma^2)$ is added to the original signal, where σ^2 is fixed to 1 and E in (14) is scaled to a certain SNR level. Output SNR is also used as a metric to evaluate the proposed sampling. "mismatch setting1" and "mismatch setting2" are the same as those of the third experiment.

It is shown in Figure 12 that the results obtained by using the QPSK signal as the test signal are quite similar to the results from the third experiment. The SNR of the reconstructed signal of the proposed serial MCS is improved as the increase of the SNR of input signal. However, when the SNR of input signal is greater than 20dB, the SNR of the reconstructed signal of the traditional parallel MCS is not improved as the increase of the SNR of input signal. The reason is that, with the increase of SNR of input signal, or, the increase of the amplitude of original signal, the mismatch error among channels becomes salient.

5. Conclusion

A serial MCS is proposed based on clocking single ADC with nonuniform clock for acquiring wideband sparse signal. The design of universal sampling pattern is also included for the proposed serial MCS. Compared with the traditional parallel MCS, the proposed serial MCS does not exist the mismatch among sub-ADCs, so higher dynamic range can be obtained. Simulation results show that the proposed serial MCS has a better reconstruction performance than the traditional parallel MCS.

Data Availability

The data used to support the findings of this study are available from the corresponding author upon request.

Conflicts of Interest

The authors declare that they have no conflicts of interest.

References

[1] M. Mishali and Y. C. Eldar, "Blind multiband signal reconstruction: compressed sensing for analog signals," *IEEE Transactions on Signal Processing*, vol. 57, no. 3, pp. 993–1009, 2009.

[2] M. Mishali and Y. C. Eldar, "From theory to practice: sub-nyquist sampling of sparse wideband analog signals," *IEEE Journal of Selected Topics in Signal Processing*, vol. 4, no. 2, pp. 375–391, 2010.

[3] T. Moon, H. W. Choi, N. Tzou, and A. Chatterjee, "Wideband Sparse Signal Acquisition with Dual-rate Time-Interleaved Undersampling Hardware and Multicoset Signal Reconstruction Algorithms," *IEEE Transactions on Signal Processing*, vol. 63, no. 24, pp. 6486–6497, 2015.

[4] P. Feng and Y. Bresler, "Spectrum-blind minimum-rate sampling and reconstruction of multiband signals," in *Proceedings of the 1996 IEEE International Conference on Acoustics, Speech, and Signal Processing, ICASSP. Part 1 (of 6)*, pp. 1688–1691, May 1996.

[5] Y. Zhao, Y. Hen Hu, and J. Liu, "Random triggering-based sub-nyquist sampling system for sparse multiband signal," *IEEE Transactions on Instrumentation and Measurement*, vol. 66, no. 7, pp. 1789–1797, 2017.

[6] Y. Zhao, X. Zhuang, H. Wang, and Z. Dai, "Sub-Nyquist sampling of high-speed repetitive waveforms using compressed sensing," *Journal of Scientific and Industrial Research*, vol. 70, no. 2, pp. 118–122, 2011.

[7] K. Chandrasekhar, D. V. Ingale, S. G. T. Moorthy, and K. V. Lakshmeesha, "Eigenvector based wideband spectrum sensing with sub-Nyquist sampling for cognitive radio," *Journal of Scientific and Industrial Research*, vol. 76, pp. 535–539, 2017.

[8] M. E. Domínguez-Jiménez, N. González-Prelcic, G. Vazquez-Vilar, and R. López-Valcarce, "Design of universal multicoset sampling patterns for compressed sensing of multiband sparse signals," in *Proceedings of the IEEE International Conference on Acoustics, Speech, and Signal Processing, ICASSP '12*, pp. 3337–3340, March 2012.

[9] I. Orovic, V. Papic, C. Ioana, M. X. Li, and S. Stankovic, "Compressive sensing in signal processing: algorithms and transform domain formulations," *Mathematical Problems in Engineering*, vol. 2016, Article ID 7616393, 16 pages, 2016.

[10] H.-H. Chen, J. Lee, and J.-T. Chen, "Digital background calibration for timing mismatch in time-interleaved ADCs," *IEEE Electronics Letters*, vol. 42, no. 2, pp. 74-75, 2006.

[11] K. J. Yang, J. L. Shi, S. L. Tian, W. H. Huang, and P. Ye, "Timing skew calibration method for TIADC-based 20 GSPS digital storage oscilloscope," *Journal of Circuits, Systems and Computers*, vol. 25, Article ID 1650007, 2016.